SSD1 suppresses phenotypes induced by the lack of Elongator-dependent tRNA modifications

Fu Xu, Anders S. Byström*, Marcus J.O. Johansson*

Department of Molecular Biology, Umeå University, 901 87 Umeå, Sweden

* Corresponding author

E-mail: marcus.johansson@umu.se or anders.bystrom@umu.se

Abstract

The Elongator complex promotes formation of 5-methoxycarbonylmethyl (mcm^5) and 5-carbamoylmethyl (ncm^5) side-chains on uridines at the wobble position of cytosolic eukaryotic tRNAs. In all eukaryotic organisms tested to date, the inactivation of Elongator not only leads to the lack of mcm^5/ncm^5 groups in tRNAs, but also a wide variety of phenotypes. Although the phenotypes are most likely caused by a translational defect induced by reduced functionality of the hypomodified tRNAs, the mechanism(s) underlying individual phenotypes are poorly understood. In this study, we show that the genetic background modulates the phenotypes induced by the lack of mcm^5/ncm^5 groups in *Saccharomyces cerevisiae.* We show that the stress-induced growth defects of Elongator mutants are stronger in the W303 than in the closely related S288C genetic background and that the phenotypic differences are caused by the known polymorphism at the locus for the mRNA binding protein Ssd1. Moreover, the mutant *ssd1* allele found in W303 cells is required for the reported histone H3 acetylation and telomeric gene silencing defects of Elongator mutants. The difference at the *SSD1* locus also partially explains why the simultaneous lack of mcm^5 and 2-thio groups at wobble uridines is lethal in the W303 but not in the S288C background. Collectively, our results demonstrate that the *SSD1* locus modulates phenotypes induced by the lack of Elongator-dependent tRNA modifications.

Author Summary

Modified nucleosides in the anticodon region of tRNAs are important for the efficiency and fidelity of translation. The Elongator complex promotes formation of several related modified uridine residues at the wobble position of eukaryotic tRNAs.

In yeast, plants, worms, mice and humans, mutations in genes for Elongator subunits lead to a wide variety of different phenotypes. Here, we show that the genetic background modulates the phenotypic consequences of the inactivation of budding yeast Elongator. This background effect is largely a consequence of a polymorphism at the *SSD1* locus, encoding a RNA binding protein that influences translation, stability and/or localization of mRNAs. We show that several phenotypes reported for yeast Elongator mutants are either significantly stronger or only detectable in strains harboring a mutant *ssd1* allele. Thus, *SSD1* is a suppressor of the phenotypes induced by the hypomodification of tRNAs.

Introduction

A general feature of tRNA molecules is that a subset of their nucleosides harbors post-transcriptional modifications. Modified nucleosides are frequently found in the anticodon region of tRNAs, especially at position 34 (the wobble nucleoside) and 37. Modifications at these positions typically influence the decoding properties of tRNAs by improving or restricting anticodon-codon interactions [1, 2]. Uridines present at the wobble position in eukaryotic cytoplasmic tRNAs often harbor a 5-methoxycarbonylmethyl (mcm^5) or 5-carbamoylmethyl (ncm^5) side-chain and sometimes also a 2-thio (s^2) or 2'-*O*-methyl group [3, 4]. The first step in the synthesis of the mcm^5 and ncm^5 side-chains requires the Elongator complex, which is composed of six Elp proteins (Elp1-Elp6) [5-9]. Elongator is thought to catalyze the addition of a carboxymethyl (cm) group to the 5-position of the uridine which is then converted to mcm^5 by the Trm9/Trm112 complex or to ncm^5 by a yet unidentified mechanism [5, 8-12].

In the budding yeast *Saccharomyces cerevisiae*, the inactivation of any of the six *ELP* genes (*ELP1-ELP6*) not only leads to the lack of the mcm^5/ncm^5 groups but also slower growth rate and numerous additional phenotypes [5, 13]. These phenotypes include increased sensitivity to elevated temperatures and various chemical stresses as well as defects in transcription, exocytosis, telomeric gene silencing, and protein homeostasis [14-18]. Even though Elongator mutants lack mcm^5/ncm^5 groups in 11 tRNA species [5, 19], the pleiotropic phenotypes are suppressed by increased expression of various combinations of the hypomodified forms of the three tRNA species that normally harbor a $mcm^5s^2U_{34}$ residue, $tRNA^{Lys}_{UUU}$, $tRNA^{Gln}_{UUG}$ and $tRNA^{Glu}_{UUC}$ [18, 20, 21]. These findings suggest the pleiotropic phenotypes of Elongator mutants are caused by a reduced functionality of the

82 hypomodified $tRNA^{Lys}_{UUU}$, $tRNA^{Gln}_{UUG}$ and $tRNA^{Glu}_{UUC}$ in translation [20, 21]. The
83 importance of the modified wobble residue in these tRNAs was supported by the
84 finding that strains lacking the s^2 group show the same but slightly weaker
85 phenotypes that are also suppressed by increased expression of the three tRNAs
86 [20, 21]. Moreover, ribosome profiling experiments have shown that the inactivation
87 of Elongator causes an accumulation of ribosomes with AAA, CAA or GAA codons in
88 the ribosomal A-site [18, 22, 23]. However, the pausing at the codons appears to be
89 relatively small [18, 22] and the mechanism(s) underlying the pleiotropic phenotypes
90 of Elongator mutants are poorly understood.

91 In yeast, the cell wall stress that arises during normal growth or through
92 environmental challenges is sensed and responded to by the cell wall integrity (CWI)
93 pathway [24, 25]. The CWI pathway is induced by several different types of stresses,
94 including growth at elevated temperatures, hypo-osmotic shock, and exposure to
95 various cell wall stressing agents [25]. A family of cell surface sensors (Wsc1-Wsc3,
96 Mid2 and Mtl1) detects the cell wall stress and recruits the guanine nucleotide
97 exchange factors Rom1 and Rom2 which activate the small GTPase Rho1. Rho1-
98 GTP binds and activates several effectors, including the kinase Pkc1. Pkc1 activates
99 a downstream MAP kinase cascade comprised of the MAPKKK Bck1, the two
100 redundant MAPKK Mkk1 and Mkk2, and the MAPK Mpk1 (Slt2). The phosphorylated
101 Mpk1 then activates factors that promote transcription of genes important for cell wall
102 biosynthesis and remodeling.

103 In addition to the CWI pathway, several other factors and pathways are known
104 to influence the cell wall remodeling that occurs upon stress, e.g. the mRNA-binding
105 protein Ssd1. Ssd1 has been reported to bind and influence the translation, stability
106 and/or localization of a subset of cellular mRNAs of which many encode proteins

107 important for cell wall biosynthesis and remodeling, [26-31]. The wild-type *SSD1*
108 gene was originally identified as a suppressor of the lethality induced by a deletion of
109 the *SIT4* gene, which encodes a phosphatase involved in a wide range of cellular
110 processes [32]. The study also led to the finding that some wild-type *S. cerevisiae*
111 laboratory strains harbor a mutation at the *SSD1* locus that is synthetic lethal with
112 the *sit4Δ* allele [32]. The *SSD1* locus has since been genetically implicated in many
113 cellular processes, including cell wall integrity, various signal transduction pathways,
114 cell morphogenesis, cellular aging, virulence, and transcription by RNA polymerase I,
115 II and III [33-38]. Although the mechanisms by which Ssd1 influences these
116 processes are poorly understood, they possibly involve both direct and indirect
117 effects of Ssd1´s influence on messenger ribonucleoprotein (mRNP) complexes [28,
118 29, 39]. With respect to the transcripts that encode cell wall remodeling factors, Ssd1
119 seems to act as a translational repressor and this function is controlled by the protein
120 kinase Cbk1, which is a component in the RAM (Regulation of Ace2 and cellular
121 morphogenesis) network [28]. In addition to relieving the translational repression, the
122 phosphorylation of Ssd1 appears to promote polarized localization of some Ssd1-
123 associated mRNAs [28, 31].
124 In this study, we show that increased activation of the CWI signaling pathway
125 counteracts the temperature sensitive (Ts) growth defect of *elp3Δ* mutants in the
126 W303 but not in the S288C genetic background. Further, the stress-induced growth
127 phenotypes caused by the tRNA modification defect are generally stronger in W303-
128 than in S288C-derived strains. We show that the phenotypic differences are due to
129 the allelic variation at the *SSD1* locus, i.e. the phenotypes are aggravated by the
130 nonsense *ssd1-d2* allele found in the W303 background. We also show that the
131 phenotypes linking the tRNA modification defect to histone acetylation and telomeric

132 gene silencing are caused by a synergistic interaction with the *ssd1-d2* allele. The
133 difference at the *SSD1* locus also provide a partial explanation to the finding [18, 40,
134 41] that cells lacking both the mcm^5 and s^2 group are viable in the S288C but not in
135 the W303 background.

136 **Results**

137 **The Ts phenotype of W303-derived *elp3Δ* cells is partially suppressed by**
138 **increased expression of factors in the CWI signaling pathway**

139 The observation that Elongator mutants are sensitive to cell wall stressing agents,
140 e.g. calcofluor white and caffeine, implies a defect in cell wall integrity [14]. This
141 notion is further supported by the finding that the Ts growth defect of Elongator-
142 deficient cells is partially suppressed by osmotic support (1 M sorbitol) [42]. As the
143 caffeine sensitivity and Ts growth defect are suppressed by increased levels of the
144 hypomodified $tRNA^{Lys}_{UUU}$ and $tRNA^{Gln}_{UUG}$ [20], the phenotypes are likely caused by
145 reduced functionality of these tRNAs in translation. To further define the wall integrity
146 defect in Elongator mutants, we determined, in the W303 genetic background, if the
147 Ts phenotype of *elp3Δ* cells is suppressed by increased expression of factors in the
148 CWI signaling pathway. The analyses revealed that the introduction of a high-copy
149 *MID2*, *WSC2*, *ROM1,* or *PKC1* plasmid into the *elp3Δ* strain partially suppressed the
150 growth defect at 37°C (Fig 1A**)**. No suppression of the phenotype was observed
151 when the cells carried a high-copy *RHO1, BCK1* or *MPK1* plasmid (Fig 1A**)**. As the
152 overexpression of neither the upstream GTPase (Rho1) nor the downstream kinases
153 (Bck1 and Mpk1) suppressed the Ts phenotype, we considered the possibility that
154 the levels of these factors may be too high when expressed from a high-copy
155 plasmid. Accordingly, low-copy *RHO1, BCK1* and *MPK1* plasmids suppress the Ts
156 phenotype of *elp3Δ* cells to a level similar to that observed for the high-copy *MID2*,
157 *WSC2*, *ROM1,* and *PKC1* plasmids (Fig 1A). The level of suppression is, however,
158 smaller than that observed for increased *tK(UUU)* and *tQ(UUG)* dosage, encoding
159 $tRNA^{Lys}_{UUU}$ and $tRNA^{Gln}_{UUG}$, respectively (Fig 1A).

160 Since the Ts phenotype of *elp3Δ* cells is counteracted by elevated $tRNA^{Lys}_{UUU}$
161 and $tRNA^{Gln}_{UUG}$ levels [20], it was possible that the activation of the CWI pathway leads
162 to an increase in their relative abundance. To investigate this possibility, we used
163 northern blotting to analyze the effect of increased *PKC1* dosage on the levels of
164 $tRNA^{Lys}_{UUU}$ and $tRNA^{Gln}_{UUG}$ in *elp3Δ* cells grown at either 30°C or 37°C. The blots were
165 also probed for $tRNA^{Met}_{i}$, which served as the loading control. In contrast to the ≈2.5-
166 fold increase in $tRNA^{Lys}_{UUU}$ and $tRNA^{Gln}_{UUG}$ levels induced by increased *tK(UUU)* and
167 *tQ(UUG)* dosage (Fig 1B and S1 Table), the abundance of the tRNAs were largely
168 unaffected by increased *PKC1* dosage at both 30°C and 37°C (Fig 1B and S1 Table).
169 Collectively, our results suggest that the Ts phenotype of *elp3Δ* cells is, at least in
170 the W303 genetic background, partially suppressed by increased activation of the
171 CWI signaling pathway.
172

173 **The allelic variant at the *SSD1* locus modulates the growth phenotypes of**
174 ***elp3Δ* cells**

175 Phenotypes caused by a mutation in an individual gene can be modulated by the
176 genetic background of the cell. In fact, the Ts phenotype induced by an *elp3Δ* allele
177 is more pronounced in strains derived from W303 than in those from S288C (Fig 2A).
178 As the inactivation of Elongator causes a lack of wobble mcm^5/ncm^5 groups in both
179 strain backgrounds [5, 43], the Ts phenotype is likely modulated by genetic variation
180 between W303 and S288C. The difference in phenotype (Fig 2A) prompted us to
181 investigate if increased *MID2*, *WSC2*, *ROM1, RHO1, PKC1, BCK1* or *MPK1* dosage
182 counteracts the Ts phenotype of *elp3Δ* cells in the S288C background. The analyses
183 showed that none of the plasmids counteracted the phenotype (S1A Fig). Moreover,
184 the growth defect of *elp3Δ* cells at 37°C is counteracted by osmotic support (1 M

185 sorbitol) in the W303, but not in the S288C background (S1B Fig). Importantly, the
186 Ts phenotype of *elp3Δ* cells is suppressed by increased *tK(UUU)* and *tQ(UUG)*
187 dosage in both genetic backgrounds (Fig 1A and S1A Fig), showing that the
188 underlying cause is the hypomodified $tRNA^{Lys}_{UUU}$ and $tRNA^{Gln}_{UUG}$. We conclude that the
189 genetic background influences the phenotypes linking the tRNA modification defect
190 to cell wall integrity.

191 Although W303 is closely related to S288C, comparisons of the genomes
192 identified polymorphisms in ≈800 genes that lead to variations in the amino acid
193 sequence [44, 45]. To identify the cause of the phenotypic differences between the
194 *elp3Δ* strains, we examined polymorphisms that have been shown to be
195 physiologically relevant. The polymorphism at the *SSD1* locus was a good candidate
196 as *SSD1* has been genetically implicated in many cellular processes, including the
197 maintenance of cellular integrity [32, 33, 46-50]. Ssd1 is a RNA binding protein that
198 associates with a subset of mRNAs of which many encode proteins important for cell
199 wall biosynthesis and remodeling [26-28]. The *SSD1* allele in the S288C background
200 encodes the full-length Ssd1 protein (1250 amino acids) whereas the allele in W303,
201 designated *ssd1-d2,* contains a nonsense mutation that introduces a premature stop
202 codon at the 698th codon of the open reading frame [32, 35]. To investigate if the
203 allele at the *SSD1* locus contributes to the phenotypic differences between the *elp3Δ*
204 mutants, we analyzed congenic *ssd1-d2, SSD1, ssd1-d2 elp3Δ*, and *SSD1 elp3Δ*
205 strains in both strain backgrounds. HPLC analyses of the nucleoside composition of
206 total tRNA from these strains showed that the levels of ncm^5U, mcm^5U, and
207 mcm^5s^2U are comparable in the *ssd1-d2* and *SSD1* strains and not detectable in the
208 *ssd1-d2 elp3Δ* and *SSD1 elp3Δ* mutants (S2 Table). The HPLC analyses also
209 showed that the allele at the *SSD1* locus does not appear to influence the

210 abundance of other modified nucleosides present in tRNAs (S2 Fig). By analyzing
211 the growth of the strains, we found that the *ssd1-d2* allele augments the Ts
212 phenotype of *elp3*Δ cells in both backgrounds (Fig 2B and S3 Table). The *ssd1-d2*
213 allele also appears to cause a slightly reduced growth rate of strains with a wild-type
214 *ELP3* gene at the elevated temperature (S3 Table). Even though the *elp3Δ* mutants
215 grow slower than the *ELP3* strains at 30°C, the effect of the *ssd1-d2* allele is less
216 pronounced at that temperature (S3 Table). In both genetic backgrounds, the
217 increased activation of the CWI signaling pathway, through increased *PKC1* dosage,
218 suppresses the Ts phenotype of the *ssd1-d2 elp3Δ*, but not the *SSD1 elp3Δ* strains
219 (Fig 2C). Although the *elp3Δ* strains show increased sensitivity to caffeine,
220 irrespective of the allele at the *SSD1* locus, the *ssd1-d2 elp3Δ* cells are in both
221 backgrounds more caffeine-sensitive than the *SSD1 elp3Δ* cells (Fig 2D). This
222 observation is consistent with the previous finding that the *ssd1-d2* allele enhances
223 the growth inhibitory effects of caffeine [32].

224 The inactivation of Elongator not only leads to increased sensitivity to caffeine,
225 but also to other stress-inducing agents [14, 17, 18]. To investigate if the *ssd1-d2*
226 allele influences these phenotypes, we analyzed the growth of the *ssd1-d2, SSD1,*
227 *ssd1-d2 elp3Δ*, and *SSD1 elp3Δ* strains on medium containing rapamycin,
228 hydroxyurea or diamide. The analyses revealed that the *ssd1-d2* allele, irrespective
229 of background, also increases the sensitivity of *elp3Δ* cells to these compounds (Fig
230 2D). Northern blot analyses revealed that the relative abundance of $tRNA^{Lys}_{UUU}$ and
231 $tRNA^{Gln}_{UUG}$ is largely unaffected by allelic variant at the *SSD1* locus (S3 Fig and S4
232 Table), indicating that the *ssd1-d2* allele influences the phenotypes by a different
233 mechanism. Collectively, these results show that the allele at the *SSD1* locus
234 influences stress-induced growth defects of *elp3Δ* cells.

235

236 **The *ssd1-d2* allele is required for the histone acetylation and telomeric gene**
237 **silencing defects of *elp3Δ* mutants**

238 In the W303 background, *elp3Δ* mutants show reduced acetylation of histone H3 [15].
239 Although the phenotype was originally thought to reflect a function of Elongator in
240 RNA polymerase II transcription [15], the reduced acetylation of lysine-14 (K14) in
241 histone H3 was subsequently shown to be an indirect consequence of the tRNA
242 modification defect [20]. To investigate if the *ssd1-d2* allele contributes to the
243 phenotype, we analyzed, in the W303 background, the histone H3 K14 acetylation
244 levels in the *ssd1-d2, ssd1-d2 elp3Δ, SSD1,* and *SSD1 elp3Δ* strains. As previously
245 shown [15, 20], the level of K14 acetylation is lower in the *ssd1-d2 elp3Δ* mutant
246 than in the *ssd1-d2* strain (Fig 3A). However, the *SSD1* and *SSD1 elp3Δ* strains
247 show comparable levels of K14 acetylated histone H3, indicating that it is the
248 combination of the *elp3Δ* and *ssd1-d2* alleles that induces the histone H3 acetylation
249 defect.

250 W303-derived Elongator mutants have also been reported to show delayed
251 transcriptional activation of the *GAL1* and *GAL10* genes upon a shift from raffinose-
252 to galactose-containing medium [20, 51]. To determine if the *ssd1-d2* allele
253 influences this phenotype, we analyzed the induction of the *GAL1* mRNA in the
254 W303-derived *ssd1-d2, ssd1-d2 elp3Δ, SSD1,* and *SSD1 elp3Δ* strains.
255 Unexpectedly, we observed no obvious delay in the induction of *GAL1* transcripts in
256 the *elp3Δ* strains regardless of the nature of the allele at the *SSD1* locus (S4 Fig). As
257 the phenotype is thought to reflect a reduced ability of Elongator mutants to adapt to
258 new growth conditions [51], it is possible that differences in media or the handling of

259 the cultures can explain why *elp3Δ* cells show rapid *GAL1* induction in our
260 experiments.

261 Another phenotype reported for Elongator mutants in the W303 background is
262 a defect in telomeric gene silencing [17, 21]. The telomere silencing defect of
263 Elongator mutants was inferred from experiments where the expression of a *URA3*
264 gene integrated close to the left telomere of chromosome VII was assayed [17, 21].
265 The defect in telomeric gene silencing leads to increased expression of the *URA3*
266 gene, which is scored as reduced growth on plates containing 5-fluoroorotic acid (5-
267 FOA) [17, 21]. Even though the integration of an *SSD1* allele into *ssd1-d2* cells does
268 not influence the level of telomeric gene silencing [36], the inactivation of *SSD1* does
269 increase the expression of a reporter gene at the silent mating type locus HMR [52].
270 The latter finding implies that the *ssd1-d2* allele may influence the assembly of silent
271 chromatin and consequently contribute to the silencing defect in Elongator mutants.
272 Accordingly, the introduction of a low-copy *SSD1* plasmid into the *ssd1-d2 elp3Δ*
273 *TELVIIL::URA3* strain [21] complemented the 5-FOA sensitivity to a level similar to
274 that observed with a plasmid carrying the wild-type *ELP3* gene (Fig 3B). Thus, the
275 telomeric gene silencing defect in Elongator mutants is caused by a synergistic
276 interaction between the *ssd1-d2* and *elp3Δ* alleles.

277

278 **The *ssd1-d2* allele augments phenotypes induced by the simultaneous lack of**
279 **mcm^5 and s^2 groups**

280 In the formation of $mcm^5s^2U_{34}$, Elongator promotes synthesis of the mcm^5 side-chain
281 whereas the thiolation of the 2-position is catalyzed by the Ncs2/Ncs6 complex [40,
282 43, 53-55]. The simultaneous lack of mcm^5 and s^2 groups was originally reported to
283 be lethal [40]. However, those experiments were performed in the W303 background

284 and more recent studies have shown that strains lacking both groups are viable in
285 the S288C background [18, 41]. To investigate if the allele at the *SSD1* locus
286 accounts for the difference in viability, we constructed *ssd1-d2 elp3Δ ncs2Δ* and
287 *SSD1 elp3Δ ncs2Δ* strains in both backgrounds all carrying a wild-type *ELP3* gene
288 on a low-copy *URA3* plasmid. Analyses of the strains revealed that the *elp3Δ ncs2Δ*
289 double mutant is viable in the W303 background if it encompasses a *SSD1* allele
290 (Fig 4A). In the S288C background, the *ssd1-d2 elp3Δ ncs2Δ* strain is viable but it
291 grows slower than the *SSD1 elp3Δ ncs2Δ* strain (Fig 4A; S5 Fig shows the same
292 plates after 2 days of incubation). These observations not only show that allele at the
293 *SSD1* locus influences the viability of *elp3Δ ncs2Δ* cells, but they also indicate that
294 the growth phenotypes are modulated by additional genetic factors.

295 The lack of the mcm^5 and/or s^2 groups has, in the S288C background, been
296 shown to correlate with an increased accumulation of protein aggregates [18]. This
297 effect was most pronounced in a strain lacking both groups and the phenotype was
298 suggested to be a consequence of co-translational misfolding due to slower
299 decoding of AAA and CAA codons by the hypomodified $tRNA^{Lys}_{UUU}$ and $tRNA^{Gln}_{UUG}$ [18].
300 Moreover, the increased load of aggregates during normal growth was proposed to
301 account for observation that the double mutant is impaired in clearing diamide-
302 induced protein aggregates [18]. As strains deleted for *SSD1* show a defect in the
303 disaggregation of heat-shock-induced protein aggregates [56], it seemed possible
304 that the *ssd1-d2* allele would augment the protein homeostasis defect in *elp3Δ*
305 *ncs2Δ* cells. To investigate this possibility, we isolated aggregates [18, 57] from the
306 *ssd1-d2*, *SSD1, ssd1-d2 elp3Δ ncs2Δ*, and *SSD1 elp3Δ ncs2Δ* strains. Analyses of
307 the insoluble fractions revealed that the levels of aggregated proteins are
308 comparable in the *ssd1-d2* and *SSD1* strains (Fig 4B). However, the *ssd1-d2 elp3Δ*

309 *ncs2Δ* mutant shows increased accumulation of aggregates compared to the *SSD1*
310 *elp3Δ ncs2Δ* strain (Fig 4B). Thus, the allele at the *SSD1* locus modulates the
311 protein homeostasis defect induced by the simultaneous lack of the wobble mcm^5
312 and s^2 groups.

313 **Discussion**

314 The phenotypic penetrance of a mutation is often impacted by the genetic
315 background, a phenomenon frequently observed in monogenic diseases [58, 59]. In
316 this study, we investigate the effect of genetic background on the phenotypes of *S.*
317 *cerevisiae* mutants defective in the formation of modified wobble uridines in tRNA.
318 We show that the phenotypes of Elongator mutants are augmented by the *ssd1-d2*
319 allele found in some wild-type laboratory strains. Moreover, the histone H3
320 acetylation and telomeric gene silencing defects reported for Elongator mutants are
321 only observed in cells harboring the *ssd1-d2* allele. Thus, the *ssd1-d2* allele
322 sensitizes yeast cells to the effects induced by the lack mcm^5/ncm^5 groups in U_{34}-
323 containing tRNAs.

324 Although the pleiotropic phenotypes of Elongator mutants are largely caused
325 by the reduced functionality of the hypomodified $tRNA^{Lys}_{UUU}$, $tRNA^{Gln}_{UUG}$ and $tRNA^{Glu}_{UUC}$,
326 the basis for individual phenotypes is poorly understood. Several not necessarily
327 mutually exclusive models have been proposed to explain how the lack of the
328 mcm^5/ncm^5 groups can lead to a particular phenotype. One model postulates that
329 phenotypes can be induced by inefficient translation of mRNAs enriched for AAA,
330 CAA and/or GAA codons and the consequent effects on the abundance of the
331 encoded factors [21, 60-62]. In this model, the inefficient decoding of the mRNAs
332 leads to reduced protein output without affecting transcript abundance. The
333 mechanism by which the slower decoding of the codons leads to reduced protein
334 levels is unclear, but it may involve the inhibition of translation initiation by the
335 queuing of ribosomes. Alternative models suggest that the phenotypes can be
336 caused by defects in protein homeostasis and/or by indirect effects on transcription
337 [18, 22]. The inactivation of *SSD1* not only influences translation and stability of the

338 transcripts normally bound by Ssd1, but it also leads to altered abundance of many
339 transcripts that do not appear to be Ssd1-associated [28, 39]. Thus, the effects of the
340 *ssd1-d2* allele on the phenotypes of *elp3Δ* cells could be due to either direct or
341 indirect effects on gene expression. Moreover, the ribosome profiling experiments of
342 Elongator mutants have been performed in the S288C background [18, 22, 23] and it
343 remains possible that the lack of Ssd1 influences the pausing at the AAA, CAA, and
344 GAA codons.

345 While the difference at the *SSD1* locus partially explains the nonviability of
346 *elp3Δ ncs2Δ* cells in the W303 background, the W303-derived *SSD1 elp3Δ ncs2Δ*
347 strain grows slower than the corresponding strain in the S288C background (S5 Fig).
348 Moreover, the *ssd1-d2 elp3Δ ncs2Δ* strain is viable, although with a growth defect, in
349 the S288C background. These findings indicate that the growth phenotypes of *elp3Δ*
350 *ncs2Δ* cells strains are modulated by additional genetic factors. Consistent with the
351 finding that *ssd1Δ* cells show a defect in Hsp104-mediated protein disaggregation
352 [56], the *ssd1-d2 elp3Δ ncs2Δ* strain shows increased accumulation of protein
353 aggregates compared to the *SSD1 elp3Δ ncs2Δ* strain in the S288C background. It
354 is, however, unclear if this increase is the cause or the consequence of the reduced
355 growth of the *ssd1-d2 elp3Δ ncs2Δ* strain.

356 **Materials and Methods**

357 **Yeast strains, plasmids, media and genetic procedures**

358 Strains and plasmids used in this study are listed in S5 Table and S6 Table. Yeast
359 media were prepared as described [63, 64]. The medium was where appropriate
360 supplemented with 2.5 ng/ml rapamycin (R0395, Sigma-Aldrich), 7 mM caffeine
361 (C0750, Sigma-Aldrich), 100 mM hydroxyurea (H8627, Sigma-Aldrich), 0.25 ng/ml
362 diamide (D3648, Sigma-Aldrich), or 1 mg/ml 5-fluoroorotic acid (R0812, Thermo
363 Fisher).

364 To generate *ssd1-d2* derivatives of BY4741 and BY4742 (S288C
365 background)[65], we first replaced the sequence between position 2907 and 3315 of
366 the *SSD1* ORF with a *URA3* gene PCR-amplified from pRS316 [66]. The
367 oligonucleotides used for strain constructions are described in S7 Table. The
368 generated strains were transformed with an *ssd1-d2* DNA fragment PCR-amplified
369 from W303-1A [67]. Following selection on 5-fluoroorotic acid (5-FOA)-containing
370 plates and subsequent single cell streaks, individual clones were screened for the
371 integration of *ssd1-d2* allele by PCR and DNA sequencing. The generated strains
372 (UMY4432 and UMY4433) were allowed to mate producing the homozygous *ssd1-*
373 *d2/ssd1-d2* strain (UMY4434).

374 Strains deleted for *ELP3* or *NCS2* were constructed by transforming the
375 appropriate diploid (UMY3387, UMY2836 or UMY4434) with an *elp3::KanMX4* or
376 *ncs2::KanMX4* DNA fragment PCR-amplified from UMY3269 (*elp3::KanMX4*) or
377 UMY3442 (*ncs2::KanMX4)* with appropriate homologies. Following PCR confirmation
378 of the deletion, the generated heterozygous diploids were allowed to sporulate and
379 the UMY4456 (*elp3Δ SSD1*, W303), MJY1019 (*ncs2Δ SSD1*, W303)*,* UMY4439
380 (*elp3Δ ssd1-d2*, S288C), UMY4442 (*ncs2Δ ssd1-d2*, S288C), MJY1036 (*elp3Δ*

381 *SSD1*, S288C), and MJY1021 (*ncs2Δ SSD1,* S288C) strains were obtained from
382 tetrads. The *elp3Δ ncs2Δ SSD1* mutants (MJY1058 and UMY4467) were obtained
383 from crosses between the relevant strains. The diploids used to generate the *elp3Δ*
384 *ncs2Δ ssd1-d2* strains (MJY1159 and UMY4454) were transformed with pRS316-
385 *ELP3* [40] before sporulation. MJY1159 was able to lose the plasmid generating
386 strain UMY4449.
387 To construct plasmids carrying individual genes for factors in the CWI
388 signaling pathway, we PCR-amplified the gene of interest using oligonucleotides that
389 introduce appropriate restriction sites (S7 Table). The DNA fragment was then
390 cloned into the corresponding sites of pRS425 [68] or pRS315 [66].
391
392 **RNA methods**
393 The abundance of individual tRNA species was determined in total RNA isolated
394 from exponentially growing cultures at an optical density at 600 nm (OD_{600}) of ≈0.5
395 [64]. Samples containing 10 µg of total RNA were separated on 8M urea-containing
396 8% polyacrylamide gels followed by electroblotting to Zeta-probe membranes (Bio-
397 Rad). The blots were sequentially probed for $tRNA^{Lys}_{UUU}$, $tRNA^{Gln}_{UUG}$ and $tRNA^{Met}_{i}$ using
398 ^{32}P-labeled oligonucleotides (S7 Table). Signals were detected and analyzed by
399 phosphorimaging using a Typhoon FLA 9500 biomolecular imager and Quantity One
400 software.
401 To analyze the induction of *GAL1* transcripts, cells were grown at 30°C in 50
402 ml synthetic complete (SC) medium containing 2% raffinose (SC/Raf) to OD_{600}≈0.45.
403 The culture was harvested by centrifugation at 1,500 x g for 5 min at room
404 temperature, and the cell pellet resuspended in 15 ml pre-warmed (30°C) SC/Raf
405 medium. Following reincubation in the shaking water bath for 10 min, transcription of

406 *GAL1* was induced by the addition of 1.5 ml pre-warmed 20% galactose. Aliquots
407 were harvested [64] at various time points after the addition of galactose and the cell
408 pellets frozen on dry ice. The procedures for determining mRNA levels have been
409 described [64].
410 To analyze the nucleoside composition of total tRNA, the tRNA was isolated
411 from exponentially growing cultures at OD_{600}≈0.8 [21]. The tRNA was digested to
412 nucleosides using nuclease P1 (Sigma-Aldrich, N8630) and bacterial alkaline
413 phosphatase (Sigma-Aldrich, P4252) and the hydrolysate analyzed by HPLC [69, 70].
414 The compositions of the elution buffers were as described [70] with the difference
415 that methanol concentration in buffer A was changed to 5% (v/v).
416
417 **Histone preparation and immunoblot analyses**
418 Histones were isolated from cells grown in SC medium at 30°C to OD_{600}≈0.8. Cells
419 representing 100 OD_{600} units were harvested, washed once with water, resuspended
420 in 30 ml of buffer A (0.1 mM Tris-HCl at pH 9.4, 10 mM DTT), and incubated on a
421 rotator at 30°C for 15 min. Cells were collected, washed with 30 ml buffer B (1 M
422 Sorbitol, 20 mM HEPES at pH7.4) and resuspended in 25 ml of buffer B containing
423 600 U yeast lytic enzyme. After 1 hour incubation on a rotator at 30°C, the sample
424 was mixed with 25 ml of ice-cold buffer C (1 M Sorbitol, 20 mM PIPES at pH 6.8, 1
425 mM $MgCl_2$) followed by centrifugation at 1,500 x g for 5 min. The pellet was
426 resuspended in 40 ml nuclei isolation buffer [71] and the suspension incubated with
427 gentle mixing at 4°C for 30 min. Cell debris were removed by centrifugation at 1,500
428 x g for 5 min. The supernatant was homogenized with 5 strokes in a Dounce
429 homogenizer followed by centrifugation at 20,000 x g for 10 min. Histones in the
430 pelleted nuclei were extracted by re-suspension in 5 ml of cold 0.2 M H_2SO_4 and

431 overnight incubation on a rotator at 4°C. After centrifugation at 10,000 x g for 10 min,
432 proteins in the supernatant were precipitated by adding 0.5 volumes of 100%
433 trichloroacetic and 30 min of incubation on ice. Following centrifugation, the pellet
434 was washed twice with acetone and then dissolved in 200 µl 10 mM Tris-HCl at pH
435 8.0. Fractions (10 µl) were resolved by 15% SDS-PAGE and transferred to
436 Immobilon-P (Millipore) membranes. The blots were incubated with rabbit anti-acetyl-
437 histone H3 (Lys14) antibodies (1:1,000 dilution, Millipore, 07-353) and then with
438 horseradish peroxidase-linked donkey anti-rabbit IgG (NA934, GE Healthcare). Blots
439 were stripped and reprobed with rabbit anti-histone H3 antibodes (1:5,000 dilution,
440 Millipore, 07-690). Proteins were detected using ECL Western blotting detection
441 reagents (GE Healthcare, RPN2209) and Amersham Hyperfilm ECL (GE Healthcare,
442 28906836).
443
444 **Analysis of protein aggregates**
445 Protein aggregates were analyzed in exponentially growing cultures in SC medium at
446 30°C. Cells representing 50 OD_{600} units were harvested at OD_{600}≈0.5 and protein
447 aggregates were isolated [18, 57] from samples containing 5 mg of total protein. 1/10
448 of the aggregates and 5µg of total protein were resolved on a 4-12% NuPAGE Bis-
449 Tris gel (Thermo Fisher, NP0321BOX) followed by staining with the Colloidal Blue
450 Staining Kit (Thermo Fisher, LC6025).
451
452 **Acknowledgments**
453 We thank members of M.J.'s and A.B.'s laboratories for valuable discussions.

454 **References**

455 1. Björk GR, Hagervall TG. Transfer RNA Modification: Presence, Synthesis, and
456 Function. EcoSal Plus. 2014;6. PMID: 26442937
457 2. Agris PF, Narendran A, Sarachan K, Vare VYP, Eruysal E. The Importance of
458 Being Modified: The Role of RNA Modifications in Translational Fidelity.
459 Enzymes. 2017;41: 1-50. PMID: 28601219
460 3. Machnicka MA, Olchowik A, Grosjean H, Bujnicki JM. Distribution and
461 frequencies of post-transcriptional modifications in tRNAs. RNA Biol. 2014;11:
462 1619-29. PMID: 25611331
463 4. Phizicky EM, Hopper AK. tRNA biology charges to the front. Genes Dev.
464 2010;24: 1832-60. PMID: 20810645
465 5. Huang B, Johansson MJO, Byström AS. An early step in wobble uridine tRNA
466 modification requires the Elongator complex. RNA. 2005;11: 424-36. PMID:
467 15769872
468 6. Winkler GS, Petrakis TG, Ethelberg S, Tokunaga M, Erdjument-Bromage H,
469 Tempst P, et al. RNA polymerase II elongator holoenzyme is composed of two
470 discrete subcomplexes. J Biol Chem. 2001;276: 32743-9. PMID: 11435442
471 7. Dauden MI, Jaciuk M, Muller CW, Glatt S. Structural asymmetry in the eukaryotic
472 Elongator complex. FEBS Lett. 2018;592: 502-15. PMID: 28960290
473 8. Kolaj-Robin O, Seraphin B. Structures and Activities of the Elongator Complex
474 and Its Cofactors. Enzymes. 2017;41: 117-49. PMID: 28601220
475 9. Johansson MJO, Xu F, Byström AS. Elongator-a tRNA modifying complex that
476 promotes efficient translational decoding. Biochim Biophys Acta Gene Regul
477 Mech. 2018;1861: 401-8. PMID: 29170010

478 10. Kalhor HR, Clarke S. Novel methyltransferase for modified uridine residues at
479 the wobble position of tRNA. Mol Cell Biol. 2003;23: 9283-92. PMID: 14645538
480 11. Mazauric MH, Dirick L, Purushothaman SK, Björk GR, Lapeyre B. Trm112p is a
481 15-kDa zinc finger protein essential for the activity of two tRNA and one protein
482 methyltransferases in yeast. J Biol Chem. 2010;285: 18505-15. PMID: 20400505
483 12. Chen C, Huang B, Anderson JT, Byström AS. Unexpected accumulation of
484 ncm(5)U and ncm(5)S(2) (U) in a trm9 mutant suggests an additional step in the
485 synthesis of mcm(5)U and mcm(5)S(2)U. PLoS One. 2011;6: e20783. PMID:
486 21687733
487 13. Karlsborn T, Tukenmez H, Mahmud AK, Xu F, Xu H, Byström AS. Elongator, a
488 conserved complex required for wobble uridine modifications in eukaryotes. RNA
489 Biol. 2014;11: 1519-28. PMID: 25607684
490 14. Frohloff F, Fichtner L, Jablonowski D, Breunig KD, Schaffrath R. *Saccharomyces*
491 *cerevisiae* Elongator mutations confer resistance to the *Kluyveromyces lactis*
492 zymocin. EMBO J. 2001;20: 1993-2003. PMID: 11296232
493 15. Winkler GS, Kristjuhan A, Erdjument-Bromage H, Tempst P, Svejstrup JQ.
494 Elongator is a histone H3 and H4 acetyltransferase important for normal histone
495 acetylation levels in vivo. Proc Natl Acad Sci U S A. 2002;99: 3517-22. PMID:
496 11904415
497 16. Rahl PB, Chen CZ, Collins RN. Elp1p, the yeast homolog of the FD disease
498 syndrome protein, negatively regulates exocytosis independently of
499 transcriptional elongation. Mol Cell. 2005;17: 841-53. PMID: 15780940
500 17. Li Q, Fazly AM, Zhou H, Huang S, Zhang Z, Stillman B. The elongator complex
501 interacts with PCNA and modulates transcriptional silencing and sensitivity to
502 DNA damage agents. PLoS Genet. 2009;5: e1000684. PMID: 19834596

503 18. Nedialkova DD, Leidel SA. Optimization of Codon Translation Rates via tRNA
504 Modifications Maintains Proteome Integrity. Cell. 2015;161: 1606-18. PMID:
505 26052047
506 19. Johansson MJO, Esberg A, Huang B, Björk GR, Byström AS. Eukaryotic wobble
507 uridine modifications promote a functionally redundant decoding system. Mol
508 Cell Biol. 2008;28: 3301-12. PMID: 18332122
509 20. Esberg A, Huang B, Johansson MJO, Byström AS. Elevated levels of two tRNA
510 species bypass the requirement for elongator complex in transcription and
511 exocytosis. Mol Cell. 2006;24: 139-48. PMID: 17018299
512 21. Chen C, Huang B, Eliasson M, Ryden P, Byström AS. Elongator complex
513 influences telomeric gene silencing and DNA damage response by its role in
514 wobble uridine tRNA modification. PLoS Genet. 2011;7: e1002258. PMID:
515 21912530
516 22. Zinshteyn B, Gilbert WV. Loss of a conserved tRNA anticodon modification
517 perturbs cellular signaling. PLoS Genet. 2013;9: e1003675. PMID: 23935536
518 23. Chou HJ, Donnard E, Gustafsson HT, Garber M, Rando OJ. Transcriptome-wide
519 Analysis of Roles for tRNA Modifications in Translational Regulation. Mol Cell.
520 2017;68: 978-92 e4. PMID: 29198561
521 24. Levin DE. Cell wall integrity signaling in *Saccharomyces cerevisiae*. Microbiol
522 Mol Biol Rev. 2005;69: 262-91. PMID: 15944456
523 25. Levin DE. Regulation of cell wall biogenesis in *Saccharomyces cerevisiae*: the
524 cell wall integrity signaling pathway. Genetics. 2011;189: 1145-75. PMID:
525 22174182
526 26. Uesono Y, Toh-e A, Kikuchi Y. Ssd1p of *Saccharomyces cerevisiae* associates
527 with RNA. J Biol Chem. 1997;272: 16103-9. PMID: 9195905

528 27. Hogan DJ, Riordan DP, Gerber AP, Herschlag D, Brown PO. Diverse RNA-
529 binding proteins interact with functionally related sets of RNAs, suggesting an
530 extensive regulatory system. PLoS Biol. 2008;6: e255. PMID: 18959479
531 28. Jansen JM, Wanless AG, Seidel CW, Weiss EL. Cbk1 regulation of the RNA-
532 binding protein Ssd1 integrates cell fate with translational control. Curr Biol.
533 2009;19: 2114-20. PMID: 19962308
534 29. Ohyama Y, Kasahara K, Kokubo T. *Saccharomyces cerevisiae* Ssd1p promotes
535 CLN2 expression by binding to the 5'-untranslated region of CLN2 mRNA.
536 Genes Cells. 2010;15: 1169-88. PMID: 20977549
537 30. Wanless AG, Lin Y, Weiss EL. Cell morphogenesis proteins are translationally
538 controlled through UTRs by the Ndr/LATS target Ssd1. PLoS One. 2014;9:
539 e85212. PMID: 24465507
540 31. Kurischko C, Kim HK, Kuravi VK, Pratzka J, Luca FC. The yeast Cbk1 kinase
541 regulates mRNA localization via the mRNA-binding protein Ssd1. J Cell Biol.
542 2011;192: 583-98. PMID: 21339329
543 32. Sutton A, Immanuel D, Arndt KT. The SIT4 protein phosphatase functions in late
544 G1 for progression into S phase. Mol Cell Biol. 1991;11: 2133-48. PMID:
545 1848673
546 33. Kaeberlein M, Guarente L. *Saccharomyces cerevisiae MPT5* and *SSD1* function
547 in parallel pathways to promote cell wall integrity. Genetics. 2002;160: 83-95.
548 PMID: 11805047
549 34. Wilson RB, Brenner AA, White TB, Engler MJ, Gaughran JP, Tatchell K. The
550 *Saccharomyces cerevisiae SRK1* gene, a suppressor of bcy1 and ins1, may be
551 involved in protein phosphatase function. Mol Cell Biol. 1991;11: 3369-73. PMID:
552 1645449

553 35. Jorgensen P, Nelson B, Robinson MD, Chen Y, Andrews B, Tyers M, et al. High-
554 resolution genetic mapping with ordered arrays of *Saccharomyces cerevisiae*
555 deletion mutants. Genetics. 2002;162: 1091-9. PMID: 12454058
556 36. Kaeberlein M, Andalis AA, Liszt GB, Fink GR, Guarente L. *Saccharomyces*
557 *cerevisiae SSD1-V* confers longevity by a Sir2p-independent mechanism.
558 Genetics. 2004;166: 1661-72. PMID: 15126388
559 37. Stettler S, Chiannilkulchai N, Hermann-Le Denmat S, Lalo D, Lacroute F,
560 Sentenac A, et al. A general suppressor of RNA polymerase I, II and III
561 mutations in *Saccharomyces cerevisiae*. Mol Gen Genet. 1993;239: 169-76.
562 PMID: 8510644
563 38. Wheeler RT, Kupiec M, Magnelli P, Abeijon C, Fink GR. A *Saccharomyces*
564 *cerevisiae* mutant with increased virulence. Proc Natl Acad Sci U S A. 2003;100:
565 2766-70. PMID: 12589024
566 39. Li L, Lu Y, Qin LX, Bar-Joseph Z, Werner-Washburne M, Breeden LL. Budding
567 yeast *SSD1-V* regulates transcript levels of many longevity genes and extends
568 chronological life span in purified quiescent cells. Mol Biol Cell. 2009;20: 3851-
569 64. PMID: 19570907
570 40. Björk GR, Huang B, Persson OP, Byström AS. A conserved modified wobble
571 nucleoside (mcm5s2U) in lysyl-tRNA is required for viability in yeast. RNA.
572 2007;13: 1245-55. PMID: 17592039
573 41. Klassen R, Grunewald P, Thuring KL, Eichler C, Helm M, Schaffrath R. Loss of
574 anticodon wobble uridine modifications affects tRNA(Lys) function and protein
575 levels in *Saccharomyces cerevisiae*. PLoS One. 2015;10: e0119261. PMID:
576 25747122

577 42. Jablonowski D, Frohloff F, Fichtner L, Stark MJ, Schaffrath R. *Kluyveromyces*
578 *lactis* zymocin mode of action is linked to RNA polymerase II function via
579 Elongator. Mol Microbiol. 2001;42: 1095-105. PMID: 11737649
580 43. Huang B, Lu J, Byström AS. A genome-wide screen identifies genes required for
581 formation of the wobble nucleoside 5-methoxycarbonylmethyl-2-thiouridine in
582 *Saccharomyces cerevisiae*. RNA. 2008;14: 2183-94. PMID: 18755837
583 44. Ralser M, Kuhl H, Ralser M, Werber M, Lehrach H, Breitenbach M, et al. The
584 *Saccharomyces cerevisiae* W303-K6001 cross-platform genome sequence:
585 insights into ancestry and physiology of a laboratory mutt. Open Biol. 2012;2:
586 120093. PMID: 22977733
587 45. Matheson K, Parsons L, Gammie A. Whole-Genome Sequence and Variant
588 Analysis of W303, a Widely-Used Strain of *Saccharomyces cerevisiae*. G3
589 (Bethesda). 2017;7: 2219-26. PMID: 28584079
590 46. Costigan C, Gehrung S, Snyder M. A synthetic lethal screen identifies SLK1, a
591 novel protein kinase homolog implicated in yeast cell morphogenesis and cell
592 growth. Mol Cell Biol. 1992;12: 1162-78. PMID: 1545797
593 47. Lee KS, Irie K, Gotoh Y, Watanabe Y, Araki H, Nishida E, et al. A yeast mitogen-
594 activated protein kinase homolog (Mpk1p) mediates signalling by protein kinase
595 C. Mol Cell Biol. 1993;13: 3067-75. PMID: 8386319
596 48. Mazzoni C, Zarzov P, Rambourg A, Mann C. The Slt2 (Mpk1) map kinase
597 homolog is involved in polarized cell growth in *Saccharomyces cerevisiae*. J Cell
598 Biol. 1993;123: 1821-33. PMID: 8276900
599 49. Martin H, Castellanos MC, Cenamor R, Sanchez M, Molina M, Nombela C.
600 Molecular and functional characterization of a mutant allele of the mitogen-

601 activated protein-kinase gene *SLT2*(*MPK1*) rescued from yeast autolytic mutants.
602 Curr Genet. 1996;29: 516-22. PMID: 8662190
603 50. Ibeas JI, Yun DJ, Damsz B, Narasimhan ML, Uesono Y, Ribas JC, et al.
604 Resistance to the plant PR-5 protein osmotin in the model fungus
605 *Saccharomyces cerevisiae* is mediated by the regulatory effects of SSD1 on cell
606 wall composition. Plant J. 2001;25: 271-80. PMID: 11208019
607 51. Otero G, Fellows J, Li Y, de Bizemont T, Dirac AM, Gustafsson CM, et al.
608 Elongator, a multisubunit component of a novel RNA polymerase II holoenzyme
609 for transcriptional elongation. Mol Cell. 1999;3: 109-18. PMID: 10024884
610 52. Raisner RM, Madhani HD. Genomewide screen for negative regulators of sirtuin
611 activity in *Saccharomyces cerevisiae* reveals 40 loci and links to metabolism.
612 Genetics. 2008;179: 1933-44. PMID: 18689887
613 53. Noma A, Sakaguchi Y, Suzuki T. Mechanistic characterization of the sulfur-relay
614 system for eukaryotic 2-thiouridine biogenesis at tRNA wobble positions. Nucleic
615 Acids Res. 2009;37: 1335-52. PMID: 19151091
616 54. Leidel S, Pedrioli PG, Bucher T, Brost R, Costanzo M, Schmidt A, et al.
617 Ubiquitin-related modifier Urm1 acts as a sulphur carrier in thiolation of
618 eukaryotic transfer RNA. Nature. 2009;458: 228-32. PMID: 19145231
619 55. Nakai Y, Nakai M, Hayashi H. Thio-modification of yeast cytosolic tRNA requires
620 a ubiquitin-related system that resembles bacterial sulfur transfer systems. J Biol
621 Chem. 2008;283: 27469-76. PMID: 18664566
622 56. Mir SS, Fiedler D, Cashikar AG. Ssd1 is required for thermotolerance and
623 Hsp104-mediated protein disaggregation in *Saccharomyces cerevisiae*. Mol Cell
624 Biol. 2009;29: 187-200. PMID: 18936161

625 57. Koplin A, Preissler S, Ilina Y, Koch M, Scior A, Erhardt M, et al. A dual function
626 for chaperones SSB-RAC and the NAC nascent polypeptide-associated complex
627 on ribosomes. J Cell Biol. 2010;189: 57-68. PMID: 20368618
628 58. Kammenga JE. The background puzzle: how identical mutations in the same
629 gene lead to different disease symptoms. FEBS J. 2017;284: 3362-73. PMID:
630 28390082
631 59. Hou J, van Leeuwen J, Andrews BJ, Boone C. Genetic Network Complexity
632 Shapes Background-Dependent Phenotypic Expression. Trends Genet. 2018;34:
633 578-86. PMID: 29903533
634 60. Rezgui VA, Tyagi K, Ranjan N, Konevega AL, Mittelstaet J, Rodnina MV, et al.
635 tRNA tKUUU, tQUUG, and tEUUC wobble position modifications fine-tune
636 protein translation by promoting ribosome A-site binding. Proc Natl Acad Sci U S
637 A. 2013;110: 12289-94. PMID: 23836657
638 61. Bauer F, Matsuyama A, Candiracci J, Dieu M, Scheliga J, Wolf DA, et al.
639 Translational control of cell division by Elongator. Cell Rep. 2012;1: 424-33.
640 PMID: 22768388
641 62. Fernandez-Vazquez J, Vargas-Perez I, Sanso M, Buhne K, Carmona M, Paulo E,
642 et al. Modification of tRNA(Lys) UUU by elongator is essential for efficient
643 translation of stress mRNAs. PLoS Genet. 2013;9: e1003647. PMID: 23874237
644 63. Amberg DC, Burke DJ, Strathern JN. Methods in Yeast Genetics. Cold Spring
645 Harbor, N Y: Cold Spring Harbor Laboratory Press; 2005.
646 64. Johansson MJO. Determining if an mRNA is a Substrate of Nonsense-Mediated
647 mRNA Decay in *Saccharomyces cerevisiae*. Methods Mol Biol. 2017;1507: 169-
648 77. PMID: 27832540

649 65. Brachmann CB, Davies A, Cost GJ, Caputo E, Li J, Hieter P, et al. Designer
650 deletion strains derived from *Saccharomyces cerevisiae* S288C: a useful set of
651 strains and plasmids for PCR-mediated gene disruption and other applications.
652 Yeast. 1998;14: 115-32. PMID: 9483801
653 66. Sikorski RS, Hieter P. A system of shuttle vectors and yeast host strains
654 designed for efficient manipulation of DNA in Saccharomyces cerevisiae.
655 Genetics. 1989;122: 19-27. PMID: 2659436
656 67. Fiorentini P, Huang KN, Tishkoff DX, Kolodner RD, Symington LS. Exonuclease
657 I of *Saccharomyces cerevisiae* functions in mitotic recombination in vivo and in
658 vitro. Mol Cell Biol. 1997;17: 2764-73. PMID: 9111347
659 68. Christianson TW, Sikorski RS, Dante M, Shero JH, Hieter P. Multifunctional
660 yeast high-copy-number shuttle vectors. Gene. 1992;110: 119-22. PMID:
661 1544568
662 69. Gehrke CW, Kuo KC. Ribonucleoside Analysis by Reversed-Phase High
663 Performance Liquid Chromatography. In: Gehrke CW, Kuo KC, editors. Journal
664 of Chromatography Library. Chromatography and Modification of Nucleosides
665 Analytical Methods for Major and Modified Nucleosides: HPLC, GC, MS, NMR,
666 UV and FT-IR. Amsterdam: Elsevier; 1990. pp. A3-A71.
667 70. Xu F, Zhou Y, Byström AS, Johansson MJO. Identification of factors that
668 promote biogenesis of tRNACGA(Ser). RNA Biol. 2018;15: 1286-94. PMID:
669 30269676
670 71. Edmondson DG, Smith MM, Roth SY. Repression domain of the yeast global
671 repressor Tup1 interacts directly with histones H3 and H4. Genes Dev. 1996;10:
672 1247-59. PMID: 8675011

673 72. Lu J, Huang B, Esberg A, Johansson MJO, Byström AS. The *Kluyveromyces*
674 *lactis* gamma-toxin targets tRNA anticodons. RNA. 2005;11: 1648-54. PMID:
675 16244131

676 **Supporting information**

677 **S1 Fig.** The S288C-derived *elp3Δ* strain does not appear to have cell wall integrity
678 defect. (A) Growth of the *elp3Δ* (MJY1036) strain carrying the indicated high-copy
679 (h.c.) or low-copy (l.c.) *LEU2* plasmids. Cells were grown over-night at 30°C in liquid
680 SC-leu medium, serially diluted, spotted on SC-leu plates, and incubated at 30°C or
681 37°C for 3 days. (B) The wild-type (W303-1A and BY4741) and *elp3Δ* (UMY3269
682 and MJY1036) strains were grown over-night at 30°C in liquid SC medium, serially
683 diluted, spotted on SC plates and SC plates supplemented with 1M sorbitol. The
684 plates were incubated for 3 days at 30°C or 37°C.

685

686 **S2 Fig**. HPLC analyses of the nucleoside composition of total tRNA from various
687 *ssd1-d2* and *SSD1* strains. The peaks representing ncm^5U, mcm^5U, mcm^5s^2U,
688 pseudouridine (Ψ), cytidine (C), uridine (U), guanosine (G), and adenosine (A) are
689 indicated. The asterisk indicates a peak that is a contamination from the bacterial
690 alkaline phosphatase.

691

692 **S3 Fig**. Effects of *ssd1-d2* and *SSD1* alleles on the abundance of $tRNA^{Lys}_{UUU}$ and
693 $tRNA^{Gln}_{UUG}$. Northern analysis of total RNA isolated from the *ssd1-d2* (W303-1A and
694 UMY4432), *ssd1-d2 elp3Δ* (UMY3269 and UMY4439), *SSD1* (UMY3385 and
695 BY4741), and *SSD1 elp3Δ* (UMY4456 and MJY1036) strains grown in SC medium at
696 30°C. The blot was probed for $tRNA^{Lys}_{UUU}$, $tRNA^{Gln}_{UUG}$, and $tRNA^{Met}_{i}$ using radiolabeled
697 oligonucleotides.

698

699 **S4 Fig.** The transcriptional activation of *GAL1* is not impaired in *elp3Δ* mutants.
700 Northern analysis of total RNA isolated from the *ssd1-d2* (W303-1A), *ssd1-d2 elp3Δ*

701 (UMY3269), *SSD1* (UMY3385) and *SSD1 elp3Δ* (UMY4456) strains. Cells were
702 grown in SC medium containing 2% raffinose followed by induction of *GAL1*
703 transcription by the addition of 0.1 volumes 20% galactose. Time points after the
704 addition of galactose are indicated above the lanes. The blot was probed for *GAL1*
705 transcripts using a randomly labelled DNA fragment. 18S rRNA was detected using a
706 oligonucleotide probe. The blot is a representative of two independent experiments.
707
708 **S5 Fig.** Influence of the *ssd1-d2* allele on the growth of *elp3Δ ncs2Δ* cells. The figure
709 shows a shorter incubation (2 days) of the plates in Fig. 4A.
710
711 **S1 Table.** Steady-state tRNA levels in *elp3Δ* cells carrying the indicated plasmids.
712
713 **S2 Table.** Relative amounts of ncm^5U, mcm^5U and mcm^5s^2U in total tRNA isolated
714 from various strains.
715
716 **S3 Table.** Generation times of indicated strains grown at 30°C or 37°C.
717
718 **S4 Table.** Steady-state tRNA levels in the indicated strains.
719
720 **S5 Table.** Yeast strains used in this study.
721
722 **S6 Table.** Plasmids used in this study.
723
724 **S7 Table.** Oligonucleotides used in this study.

725 **Figures**

726 **Fig 1.** Increased expression of factors in the CWI signaling pathway counteracts the
727 Ts phenotype of W303-derived *elp3Δ* cells.

728 (A) Growth of the *elp3Δ* (UMY3269) strain carrying the indicated high-copy (h.c.) or
729 low-copy (l.c.) *LEU2* plasmids. The high copy plasmid carrying the *tK(UUU)* and
730 *tQ(UUG)* genes [72] is abbreviated as h.c. *tK+tQ*. Cells were grown over-night at
731 30°C in liquid synthetic complete medium lacking leucine (SC-leu), serially diluted,
732 spotted on SC-leu plates, and incubated at 30°C or 37°C for 3 days.

733 (B) Northern analysis of total RNA isolated from *elp3Δ* (UMY3269) cells carrying the
734 indicated plasmids. The cells were grown in SC-leu medium at 30°C or 37°C. The
735 blot was probed for $tRNA^{Lys}_{UUU}$, $tRNA^{Gln}_{UUG}$ and $tRNA^{Met}_{i}$ using radiolabeled
736 oligonucleotides. $tRNA^{Met}_{i}$ serves as the loading control.

737

738 **Fig 2.** The growth phenotypes *elp3Δ* cells are modulated by the allele at the *SSD1*
739 locus.

740 (A) Growth of *elp3Δ* mutants in the W303 and S288C genetic backgrounds. The
741 wild-type (W303-1A and BY4741) and *elp3Δ* strains (UMY3269 and MJY1036) were
742 streaked on SC plates and incubated at 30°C or 37°C for 3 days.

743 (B) Effects of the *ssd1-d2*/*SSD1* alleles on the growth of *elp3Δ* strains in the W303
744 and S288C genetic backgrounds. The *ssd1-d2* (W303-1A and UMY4432), *SSD1*
745 (UMY3385 and BY4741), *ssd1-d2 elp3Δ* (UMY3269 and UMY4439) and *SSD1 elp3Δ*
746 (UMY4456 and MJY1036) strains were grown over-night at 30°C in liquid SC
747 medium, serially diluted, spotted on SC plates, and incubated at 30°C or 37°C for 3
748 days.

749 (C) Effects of increased *PKC1* dosage on the growth of *elp3Δ ssd1-d2* and *elp3Δ*
750 *SSD1* strains. The relevant strains (UMY3269,UMY4456, UMY4439, and MJY1036)
751 carrying the indicated plasmids were grown over-night at 30°C in liquid SC-leu
752 medium, serially diluted, spotted on SC-leu plates, and incubated for 3 days at 30°C
753 or 37°C.
754 (D) Influence of the *ssd1-d2* allele on growth phenotypes induced by various stress-
755 inducing agents. The strains from B were grown over-night at 30°C in liquid SC
756 medium, serially diluted, spotted on SC plates and SC plates supplemented with
757 caffeine, rapamycin, hydroxyurea or diamide. The plates were incubated for 3 days
758 at 30°C.
759
760 **Fig 3.** The *ssd1-d2* allele is required for the histone acetylation and telomeric gene
761 silencing defects of *elp3Δ* cells.
762 (A) Western analysis of histones isolated from the *ssd1-d2* (W303-1A), *ssd1-d2*
763 *elp3Δ* (UMY3269), *SSD1* (UMY3385) and *SSD1 elp3Δ* (UMY4456) strains grown in
764 SC medium at 30°C. Polyclonal anti-acetyl-histone H3 and anti-histone H3
765 antibodies were used to detect the indicated proteins. The blot is a representative of
766 two independent experiments.
767 (B) Influence of the *ssd1-d2* allele on telomeric gene silencing in *elp3Δ* cells. The
768 s*sd1-d2 TELVIIL::URA3* (UMY2584) and *ssd1-d2 elp3Δ TELVIIL::URA3* (UMY3790)
769 strains carrying the indicated plasmids were grown over-night at 30°C in liquid SC-
770 leu medium, serially diluted, spotted on SC-leu and SC-leu+5-FOA plates, and
771 incubated for 3 days at 30°C.
772

773 **Fig 4.** The growth and protein homeostasis defects of *elp3Δ ncs2Δ* cells are
774 augmented by the *ssd1-d2* allele.
775 (A) Influence of the *ssd1-d2* allele on the growth of *elp3Δ ncs2Δ* cells. The s*sd1-d2*
776 *elp3Δ ncs2Δ* (UMY4454 and MJY1159) and *SSD1 elp3Δ ncs2Δ* (UMY4467 and
777 MJY1058) strains carrying the l.c. *URA3* plasmid pRS316-*ELP3* were grown over-
778 night at 30°C in SC medium, serially diluted, spotted on SC and SC+5-FOA plates,
779 and incubated for 3 days at 30°C.
780 (B) Effects of the *ssd1-d2* allele on protein aggregation in *elp3Δ ncs2Δ* cells. Total
781 protein and protein aggregates was analyzed from the *ssd1-d2* (UMY4432), *ssd1-d2*
782 *elp3Δ ncs2Δ* (UMY4449), *SSD1* (BY4741) and *SSD1 elp3Δ ncs2Δ* (MJY1058)
783 strains grown in SC medium at 30°C. The gel is a representative of two independent
784 experiments.

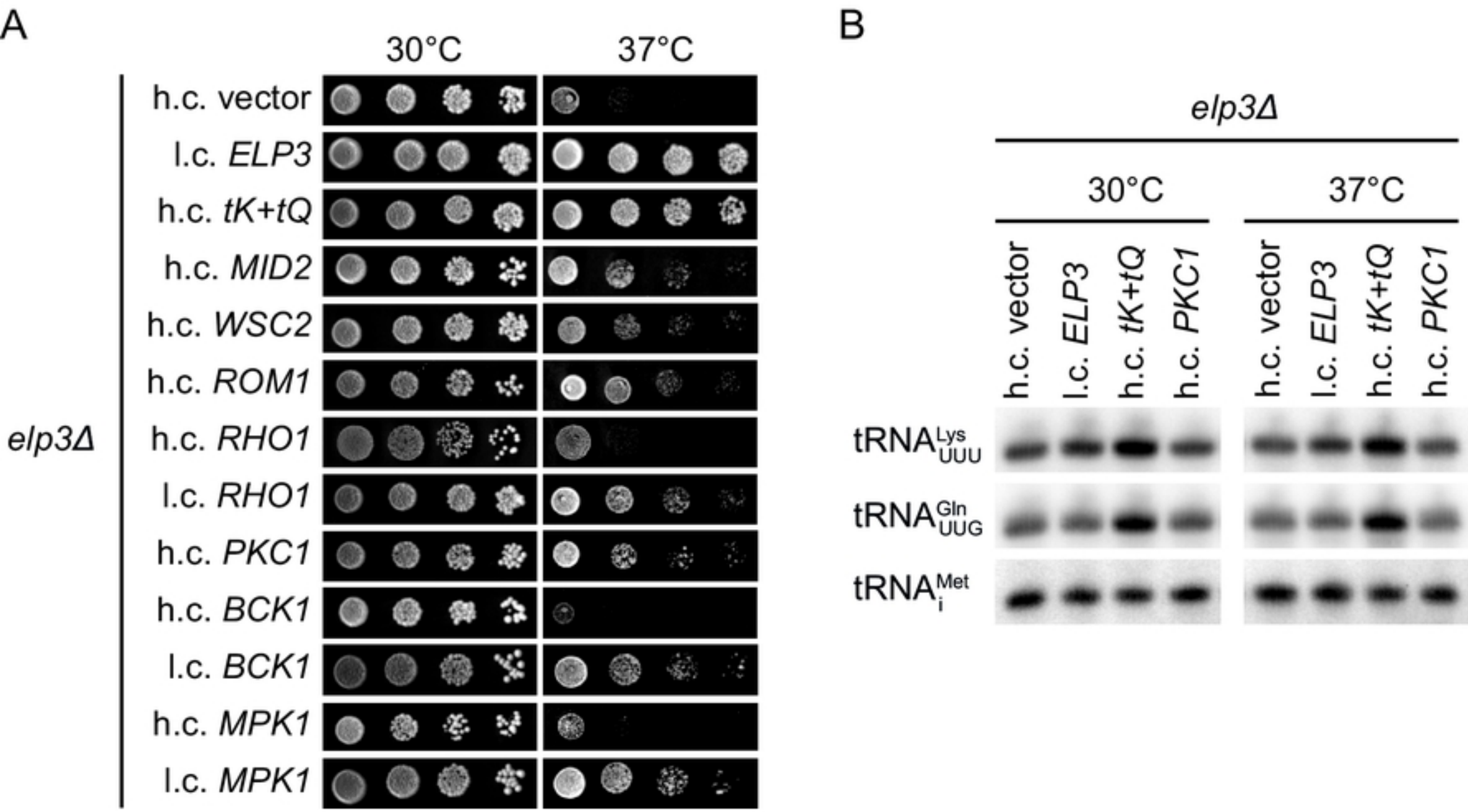
A
30°C
37°C
elp3Δ
h.c. vector
l.c. ELP3
h.c. tK+tQ
h.c. MID2
h.c. WSC2
h.c. ROM1
h.c. RHO1
l.c. RHO1
h.c. PKC1
h.c. BCK1
l.c. BCK1
h.c. MPK1
l.c. MPK1
B
elp3Δ
30°C
37°C
h.c. vector
l.c. ELP3
h.c. tK+tQ
h.c. PKC1
h.c. vector
l.c. ELP3
h.c. tK+tQ
h.c. PKC1
tRNA Lys UUU
tRNA Gln UUG
tRNA Met i

Figure 1

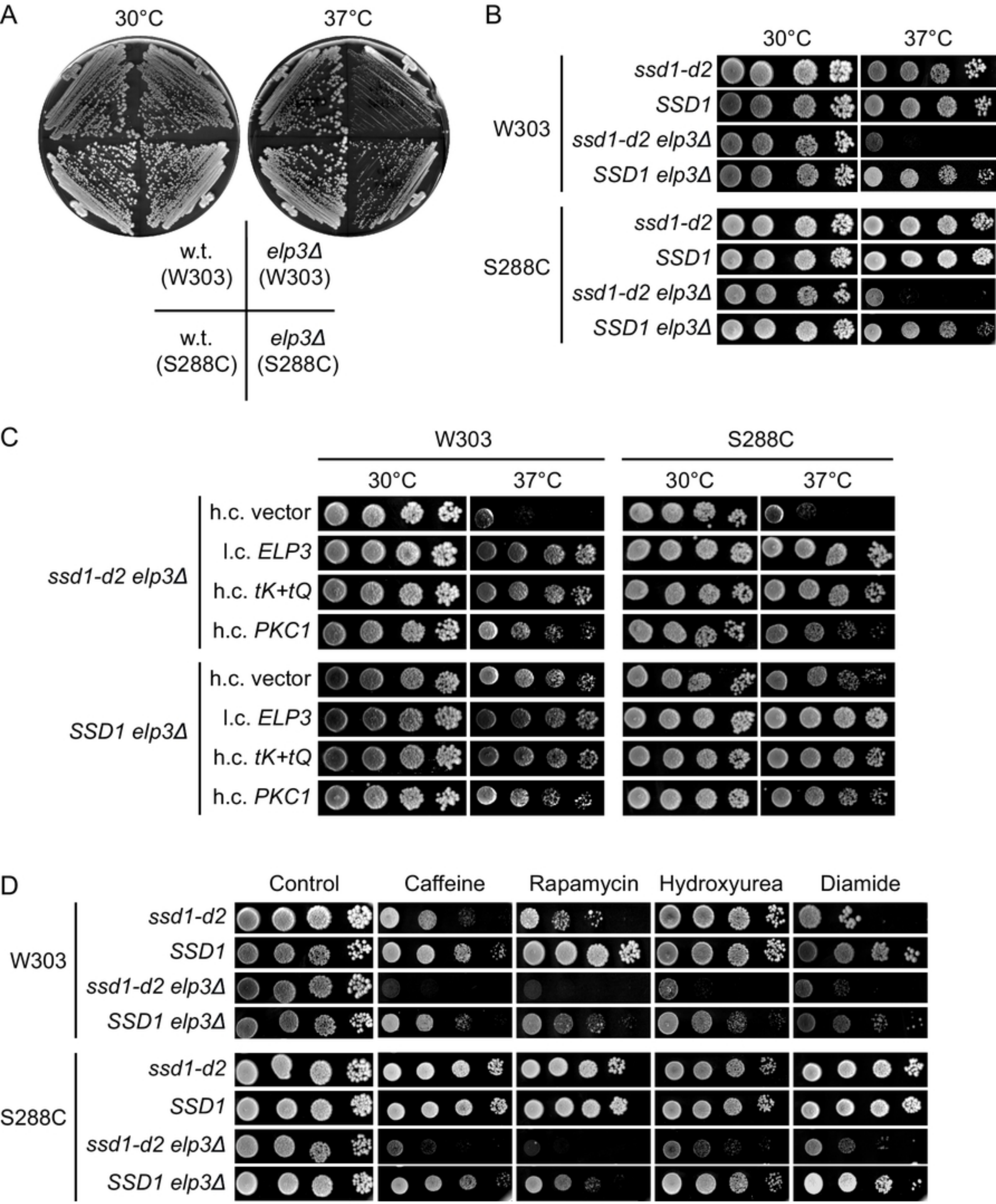
A
30°C
37°C
w.t. (W303)
elp3Δ (W303)
w.t. (S288C)
elp3Δ (S288C)
B
30°C
37°C
W303
ssd1-d2
SSD1
ssd1-d2 elp3Δ
SSD1 elp3Δ
S288C
ssd1-d2
SSD1
ssd1-d2 elp3Δ
SSD1 elp3Δ
C
W303
S288C
30°C
37°C
30°C
37°C
ssd1-d2 elp3Δ
h.c. vector
l.c. ELP3
h.c. tK+tQ
h.c. PKC1
SSD1 elp3Δ
h.c. vector
l.c. ELP3
h.c. tK+tQ
h.c. PKC1
D
Control
Caffeine
Rapamycin
Hydroxyurea
Diamide
W303
ssd1-d2
SSD1
ssd1-d2 elp3Δ
SSD1 elp3Δ
S288C
ssd1-d2
SSD1
ssd1-d2 elp3Δ
SSD1 elp3Δ

Figure 2

A

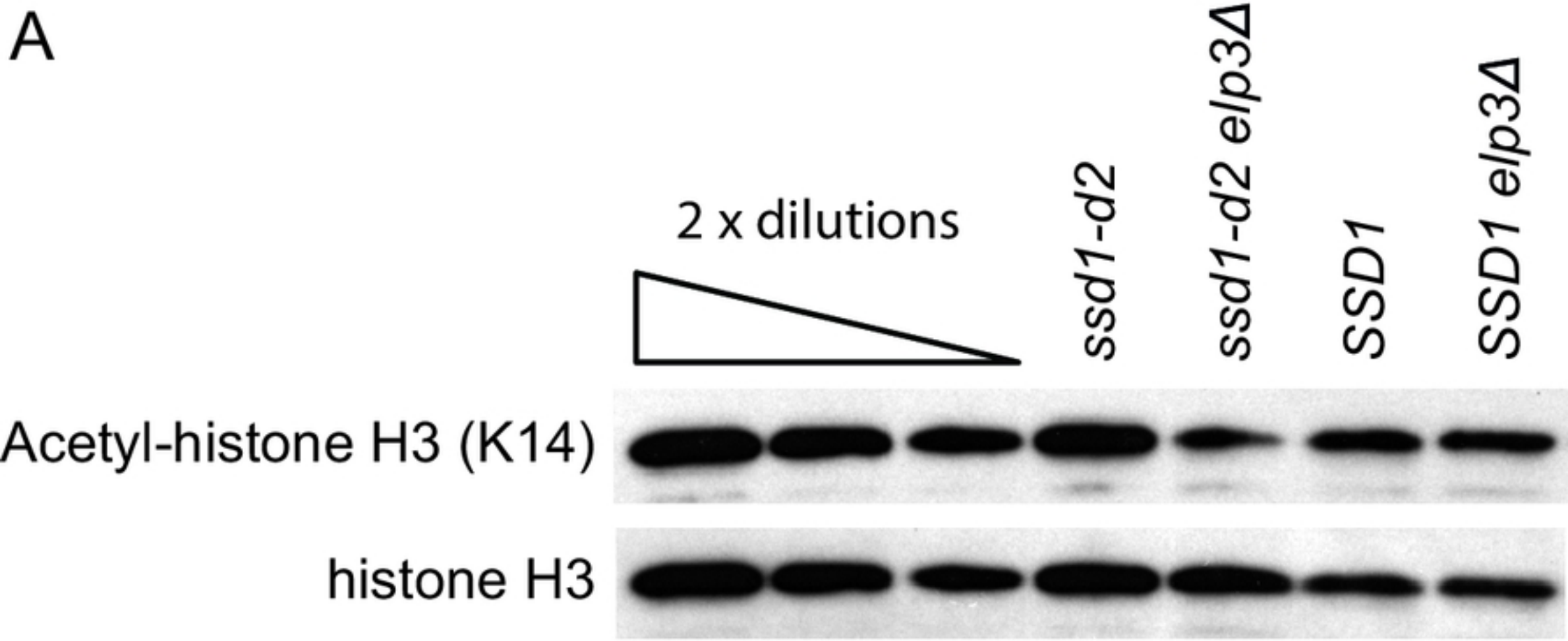
2 x dilutions
ssd1-d2
ssd1-d2 elp3Δ
SSD1
SSD1 elp3Δ
Acetyl-histone H3 (K14)
histone H3

B

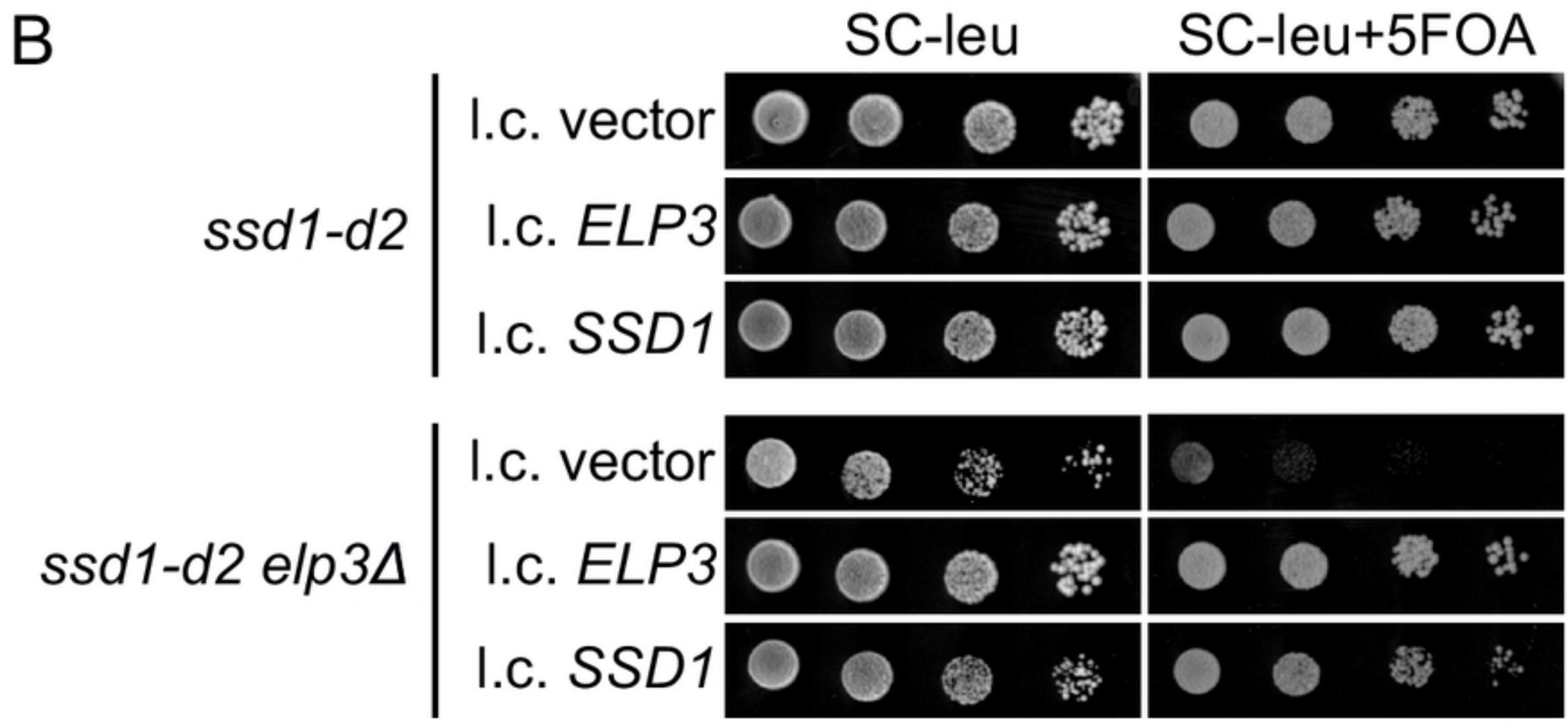
SC-leu
SC-leu+5FOA
ssd1-d2
l.c. vector
l.c. ELP3
l.c. SSD1
ssd1-d2 elp3Δ
l.c. vector
l.c. ELP3
l.c. SSD1

Figure 3

A

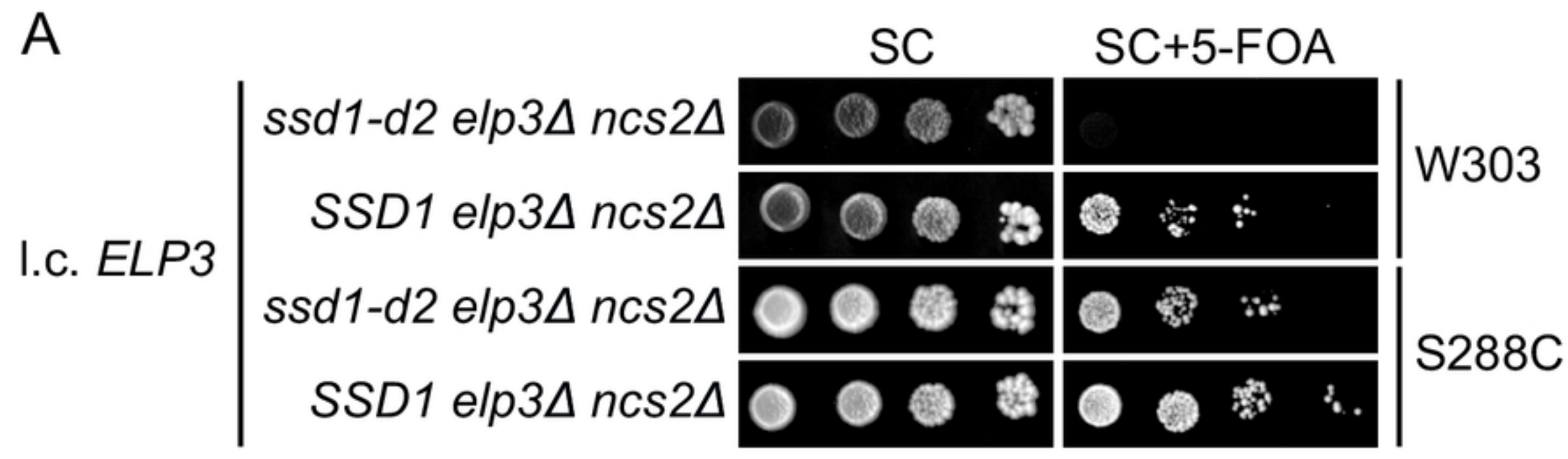
SC
SC+5-FOA
l.c. ELP3
ssd1-d2 elp3Δ ncs2Δ
SSD1 elp3Δ ncs2Δ
ssd1-d2 elp3Δ ncs2Δ
SSD1 elp3Δ ncs2Δ
W303
S288C

B

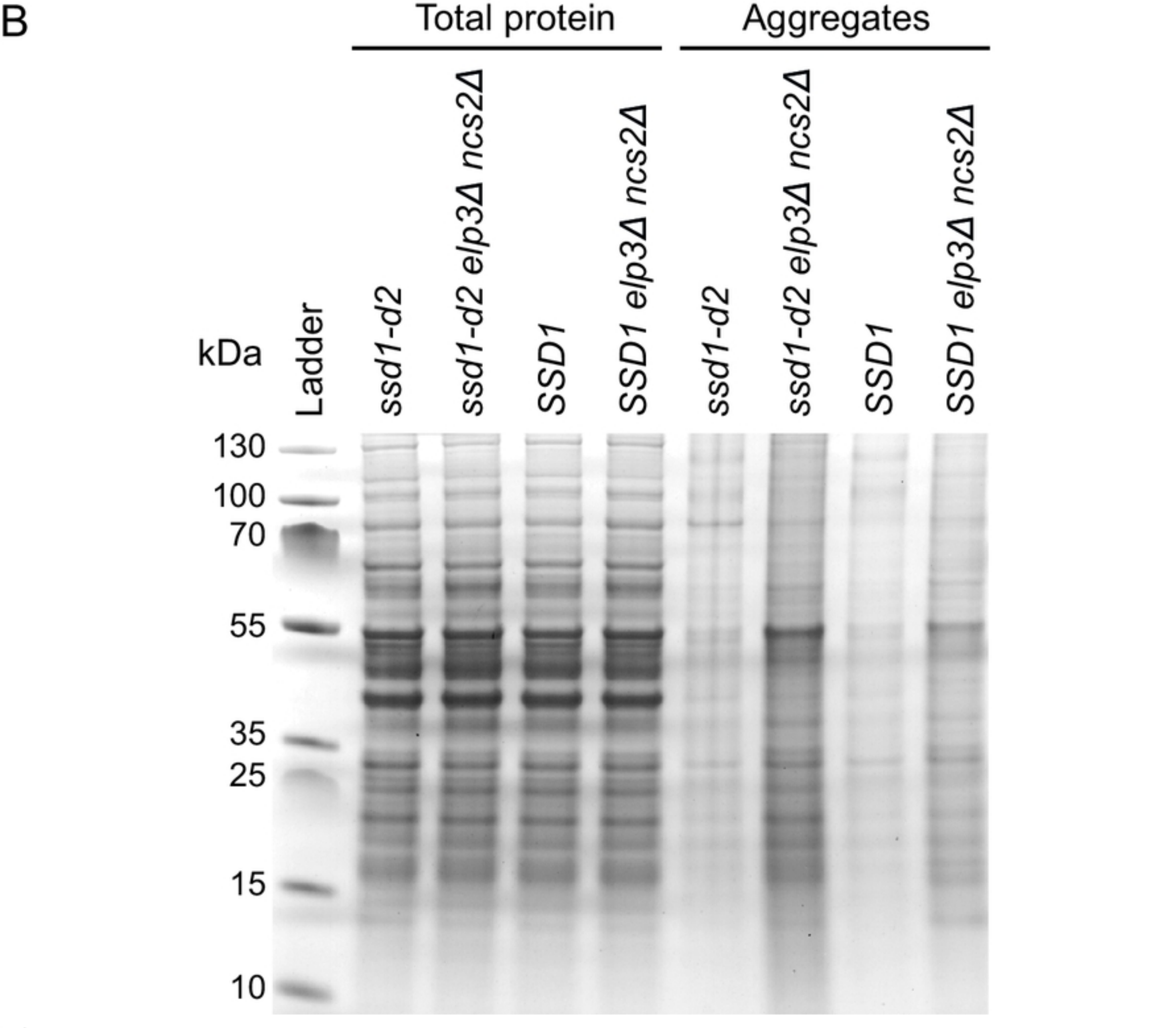
Total protein
Aggregates
kDa
Ladder
ssd1-d2
ssd1-d2 elp3Δ ncs2Δ
SSD1
SSD1 elp3Δ ncs2Δ
ssd1-d2
ssd1-d2 elp3Δ ncs2Δ
SSD1
SSD1 elp3Δ ncs2Δ
130
100
70
55
35
25
15
10

Figure 4